Multiphoton plasmon-resonance microscopy

Dvir Yelin, Dan Oron, Stephan Thiberge, Elisha Moses and Yaron Silberberg

Department of physics of Complex Systems, The Weizmann Institute of Science, Rehovot 76100, Israel

yaron.silberberg@weizmann.ac.il

Abstract: A novel method for detection of noble-metal nanoparticles by their nonlinear optical properties is presented and applied for specific labeling of cellular organelles. When illuminated by laser light in resonance with their plasmon frequency these nanoparticles generate an enhanced multiphoton signal. This enhanced signal is measured to obtain a depth-resolved image in a laser scanning microscope setup. Plasmon-resonance images of both live and fixed cells, showing specific labeling of cellular organelles and membranes, either by two-photon autofluorescence or by third-harmonic generation, are presented.

OCIS codes: (170.0110) Imaging systems; (180.5810) Scanning microscopy; (190.4160) Multiharmonic generation

References and links

1. W. C. W. Chan, S. Nie, "Quantum dot bioconjugates for ultrasensitive nonisotopic detection," Science **281**, 2016 (1998).
2. M. Bruchez Jr., M. Moronne, P. Gin, S. Weiss, A. P. Alivisatos, "Semiconductor nanocrystals as fluorescent biological labels," Science **281**, 2013 (1998).
3. S.J. Oldenburg, S.L. Westcott, R.D. Averitt, N.J. Halas, "Infrared extinction properties of gold nanoshells," J. Chem. Phys. **111**, 4729 (1999).
4. J. Aizpurua, P. Hanarp, D. S. Sutherland, M. Kall, G. W. Bryant, F. J. Garcia de Abajo, "Optical properties of gold nanorings," Phys. Rev. Lett. **90**, 057401 (2003).
5. D. Boyer, P. Tamarat, A. Maali, B. Lounis, M. Orrit, "Photothermal imaging of nanometer-sized metal particles among scatterers," Science **297**, 1160 (2002).
6. J.T. Golab, J.R. Sprague, K.T. Carron, G.C. Schatz, R.P. Van Duyne,"A Surface enhanced hyper-Raman scattering study of pyridine adsorbed onto silver: experiment and theory," J. Chem. Phys. **888**, 7942 (1988).
7. H. Kano, S. Kawata, "Two-photon-excited fluorescence enhanced by a surface plasmon," Opt. Lett. **21**, 1848 (1996).
8. B. Lamprecht, J.R. Krenn, A. Leitner, F.R. Aussenegg, "Resonant and off-resonant light-driven plasmons in metal nanoparticles studied by femtosecond-resolution third-harmonic generation," Phys. Rev. Lett. **83**, 4421 (1999).
9. G. Peleg, A. Lewis, O. Bouevitch, L. Loew, D. Parnas, M. Linial, "Gigantic optical non-linearities from nanopartical-enhanced molecular probes with potential for selectively imaging the structure and physiology of nanometric regions in cellular systems," Bioimaging **4**, 215 (1996).
10. W. Denk, J.H. Strickler, W.W. Webb, "Two-photon laser scanning fluorescence microscopy," Science **248**, 73 (1990).
11. S. Maiti, J.B. Shear, R.M. Williams, W.R. Zipfel, W.W. Webb, "Measuring serotonin distribution in live cells with three-photon excitation," Science **275**, 530 (1997).
12. D. Yelin, Y. Silberberg, "Laser scanning third-harmonic-generation microscopy in biology," Opt. Express **5**, 169 (1999).
13. M. Muller, J. Squier, K.R. Wilson, G.J. Brakenhoff,"3D-microscopy of transparent objects using third-harmonic generation," J. Microsc **191**, 266 (1998).
14. A. Zumbusch, G.R. Holtom, X.S. Xie, "Three-dimensional vibrational imaging by coherent anti-Stokes Raman scattering," Phys. Rev. Lett. **82**, 4142 (1999).
15. S. Nie, S.R. Emory, "Probing single molecules and single nanoparticles by surface-enhanced Raman scattering," Science **275**, 1102 (1997).
16. G. Peleg, A. Lewis, M. Linial, L.M. Loew, "Nonlinear optical measurement of membrane potential around single molecules at selected cellular sites," Proc. Natl. Acad. Sci. USA **96**, 6700 (1999).
17. K. Kneipp et al., "Surface-enhanced Raman spectroscopy in single living cells using gold nanoparticles," Appl. Spec. **56**, 150 (2002).

18. B. J. Messinger, K. Ulrich von Raben, R.K. Chang, P.W. Barber, "Local fields at the surface of noble metal microspheres," Phys. Rev. B **24**, 649 (1981).
19. E.J. Liang, C. Engert, W. Kiefer, "Surface-enhanced Raman scattering of pyridine in silver colloids excited in the near-infrared region," J. Raman Spec. **24**, 775 (1993).
20. M. Quinten, "Local fields close to the surface of nanoparticles and aggregates of nanoparticles," Appl. Phys. B **73**, 245 (2001).
21. D. Yelin, D. Oron, E. Korkotian, M. Segal, Y. Silberberg, "Third-harmonic microscopy with a Ti:Sapphire laser," Appl. Phys. B **74**, s97 (2002).
22. B. Alberts et al., *Molecular Biology of The Cell* (Garland Publishing Inc., New York, 1994).
23. E. Skutelsky, J. Roth, "Cationic colloidal gold - a new probe for the detection of anionic cell surface sites by electron microscopy," J. Histochemistry **34**, 693 (1986).
24. M.S. Bush, G. Allt, "Blood nerve barrier: distribution of anionic sites on the endothelial plasma membrane and basal lamina," Brain Res. **535**, 181 (1990).
25. *Concanavalin A as a Tool*, eds. H. Bittiges, H.P. Schnebli, (London, 1976).
26. R.M. Guasch, C. Guerri, J.-E. O'Connor, "Study of surface carbohydrates on isolated golgi subfractions by fluorescent-lectin binding and flow cytometry," Cytometry **19**, 112 (1995); R.M. Guasch, C. Guerri, J.-E. O'Connor, "Flow cytometric analysis of concanavalin A binding to isolate Golgi fractions from rat liver," Exp. Cell Res. **207**, 136 (1993).
27. I. Virtanen, P. Ekblom, P. Laurila, "Subcellular compartmentalization of saccharide moieties in cultured normal and malignant cells," J. Cell Biol. **85**, 429 (1980).

Recent advances in the field of nanotechnology have led to an increased interest in the design and manufacture of nanometer-sized objects which can be optically detected in the far field. Among these are core-shell semiconductor nanodots [1, 2] and shaped noble-metal nanoparticles with a tunable plasmon resonance [3, 4]. Since these nanoparticles do not suffer from photobleaching and phototoxicity, typical of organic fluorescent dyes, they are considered as attractive alternatives for specific labeling of cellular organelles in optical microscopy. The various detection methods of these nanoparticles typically rely on a linear optical process such as fluorescence, absorption or scattering. Core-shell semiconductor nanodots exhibit strong fluorescence and have been shown to be highly biocompatible [1, 2]. Recently, photothermal imaging of gold nanoparticles by means of a high-sensitivity differential interference contrast microscopy has been demonstrated [5], taking advantage of the increased linear absorption of the nanoparticle. Here we consider, in a different approach, detection of the nanoparticle by means of nonlinear optical methods. This allows intrinsic optical sectioning capabilities for the process, since the multiphoton signal is generated only at the vicinity of the focal spot, where the photon flux is high. Taking advantage of the huge enhancement of multiphoton scattering cross sections observed in proximity to metal nanoparticles illuminated by laser light in resonance with their surface plasmon [6, 7, 8, 9], we are able to demonstrate three-dimensional multiphoton imaging with average powers as low as those used in multiphoton fluorescence with organic dyes [10, 11].

In contrast with the detection methods described above, including multiphoton fluorescence, in our case the metal nanoparticle does not generate the multiphoton signal by itself, but rather acts as a nanolens, which locally amplifies the weak multiphoton processes occurring intrinsically in proximity to it. This metal nanoparticle labeling method can be used in conjunction with practically any multiphoton microscopy technique, including coherent ones, such as third-harmonic generation [12, 13] and coherent anti-Stokes Raman scattering [14], which have, up until now, been used to study unlabelled cells.

Electric field enhancement in proximity to roughened noble metal surfaces and nanoparticles has been investigated extensively both theoretically and experimentally. When the laser field frequency coincides with the surface plasmon-resonance frequency of a metal nanoparticle, huge field enhancement can be achieved. This effect has been exploited to dramatically increase the Raman scattering cross section of adsorbed molecules. Surface enhanced Raman scattering (SERS) has even enabled measurements of single molecules adsorbed on noble metal surfaces [15]. Recently, surface enhancement of both incoherent and coherent multiphoton pro-

cesses, including hyper-Raman scattering [6], multiphoton fluorescence [7] and third-harmonic generation [8], were demonstrated. In a recent experiment, the presence of gold nanoparticles at cell membranes, was shown to simultaneously enhance second-harmonic generation and to quench two-photon fluorescence from nearby dye molecules [9, 16].

Small particles, a few nanometers in diameter, can usually penetrate through cell membranes into the intra-cellular medium. Several biochemical techniques for the insertion of larger nanoparticles (60nm) into living cells are reported in a recent in-vivo spatially resolved SERS spectroscopy experiment [17]. In this work we demonstrate that plasmon resonance enhancement can indeed be combined with nonlinear microscopy for cellular imaging. The nanoparticle distribution is imaged by measuring of two different surface-enhanced multiphoton processes: two-photon autofluorescence (TPAF) and third-harmonic generation (THG), both excited by a Ti:sapphire ultrafast laser source.

Typically, the plasmon-resonance frequency of nanometer-sized metal particles is in the visible range. As the particle size increases the resonance broadens and shifts towards longer wavelengths [18]. Nanoparticles of a diameter of about 160nm are needed in order to match the plasmon-resonance of the Ti:Sapphire laser used in our experiments. This relatively large size poses a problem when attempting specific labeling with nanoparticles for multiphoton microscopy, since labeling specificity decreases with particle size (due to steric hindrance of the nanoparticle to the conjugated antibody). We address this problem by either aggregating several small nanoparticles [19, 20], or by chemical enlargement of small nanoparticles. Both these methods take advantage of the high specificity of smaller particles, while matching the resonance conditions in another manner. Neither of these methods, both relying on a stochastic process, is indeed well suited for microscopy applications. Recently, however, nano-engineered particles with a plasmon resonance at near-infrared frequencies at much smaller sizes have been introduced. These include nanoshells [3], composed of a dielectric core coated by a thin layer of metal, nanodisks and nanorings [4]. These unique nanoparticles were shown to have plasmon-resonance frequencies in the near infrared at dimensions significantly smaller than 100nm. By variation of the aspect ratio of these particles it is possible to tune the plasmon-resonance frequency, as well as the scattering and absorption cross sections in a wide range. Using the optical techniques described in our work, multiphoton optical detection of such single nanoparticles can also be achieved.

The cells used in the experiment were grown below confluency under a standard procedure on microscope cover glasses treated to favor cell adhesion. Either Chinese Hamster Ovary (CHO) cells or NIH3T3 rat kidney epithelial cells were used. A Ti:Sapphire laser, delivering 100fs pulses centered at 810nm at a repetition rate of 80MHz (spectra physics Tsunami) is used for excitation, and is focused into the sample by an oil-immersed, NA=1.4, x100 objective. The light scattered in the forward direction is collected by a UV-grade condenser, filtered by an approprtiate spectral filter and measured by a photomultiplier tube and an RF lock-in amplifier. A detailed description of the experimental system can be found in Yelin *et al.* [21].

As a first demonstration of imaging using plasmon-resonance microscopy, we image fixed CHO cells to which gold was inserted via the endocytic pathway [22]. 10nm cationic gold particles or 40nm Concanavalin-A conjugated gold particles at a concentration of 10^{10}particles/ml were added to the growing medium about 20 hours before fixation. Shown in Figs. 1(a) and (b) are TPAF images of these cells, along with a control image (Fig. 1(c)). In taking these images, a bandpass filter centered at 450nm (40nm FWHM) is used to filter the fluorescence light, and the average laser power was reduced to about 6mW to prevent local cell damage.

Cationic gold first accumulates on the negatively charged sites of the cell membrane [23, 24]. After incubation, particles are expected to accumulate in endocytic vesicles. Several bright spots are scattered in the TPAF image of a fixed cell incubated with 10nm diameter cationic gold, shown in Fig. 1(a). At these spots, the TPAF signal is enhanced by an order of magnitude compared to the background signal from the entire cell. We relate the strong TPAF signals to
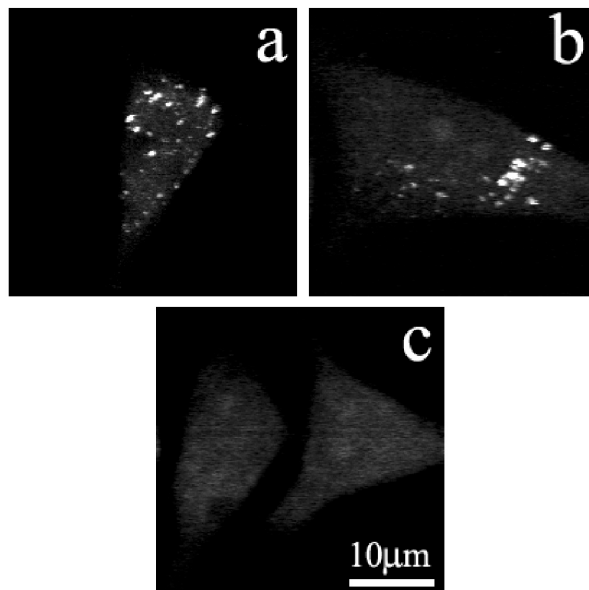
Fig. 1. Plasmon-resonance TPAF images of CHO cells incubated with (a) 10nm cationic gold.
(b) 40nm Concanavalin A gold. (c) two cells which were submitted to the same treatments per-
formed in the positive experiments (a and b), but no gold was added to the growing medium. The
strong TPAF spots in a and b are attributed to plasmon-resonance with the laser frequency where
nanoparticles are aggregated.

field enhancement by nanoparticle aggregates of a size leading to a plasmon-resonance around
800nm.

Concanavalin-A conjugated gold particles accumulate first in the extracellular matrix.
Concanavalin-A is a lectin specific for mannose-rich sugars, used for labeling of glycosylated
proteins and lipids [25]. Those are found principally in the extracellular matrix of the cell, the
endoplasmic reticulum and the Golgi apparatus. After incubation concanavalin-A conjugated
gold particles are expected to accumulate in the Golgi apparatus [26, 27]. A TPAF image of
a fixed CHO cell incubated with 40nm Concanavalin-A gold is shown in Fig. 1(b). Here too,
the strong local TPAF signals is related to nanoparticle aggregates. Several large spots are ob-
served next to the nucleus (slightly darker elliptic region in the cell), probably corresponding
to the Golgi apparatus. Numerous smaller bright spots are also visible, probably corresponding
to endocytic vesicles. We note that although some gold particles do not penetrate the cell at the
moment of fixation, and remain attached to the extracellular matrix, those particles do not form
aggregates, and thus do not enhance the TPAF at the cell membrane. Two cells from the control
experiment are shown in Fig. 1(c). These cells were submitted to the same treatment as in the
positive experiments (Figs. 1(a) and (b)), but no gold was added to the growing medium. No
bright features are observed in this relatively homogeneous TPAF image.

It should be noted that in order to validate that the enhanced signals observed in Figs. 1(a)
and (b) indeed originate from TPAF we imaged the same cell, using this time a bandpass filter
centered at 500nm (40nm FWHM), which requires that the signal frequency be shifted by over
$3500 cm^{-1}$ from the two-photon energy. While the overall signal decreased significantly, the
relative signal enhancement at the bright spots remained similar. This is indeed consistent with
a fluorescence signal. On the other hand, the large frequency shift rules out the possibility of
the signal originating from a surface-enhanced incoherent scattering process such as hyper-
Rayleigh or hyper-Raman scatterring.

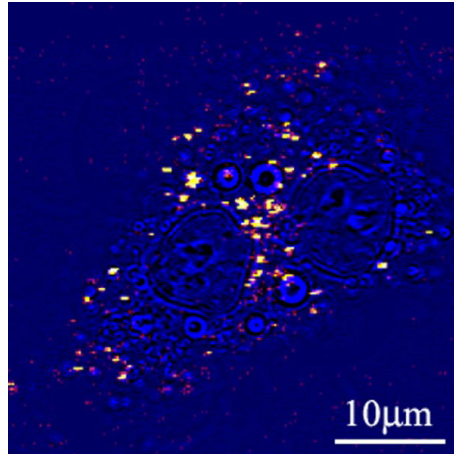A demonstration of *live* cell imaging is shown in Fig. 2. Here, 10nm cationic gold nanopar-

Fig. 2. Plasmon-resonance TPAF image of a live CHO cell incubated with 10nm cationic gold, superimposed on a simple transmission image of the cell. The transmission image is blue, while the TPAF signal goes from red (weak) to yellow (strong).
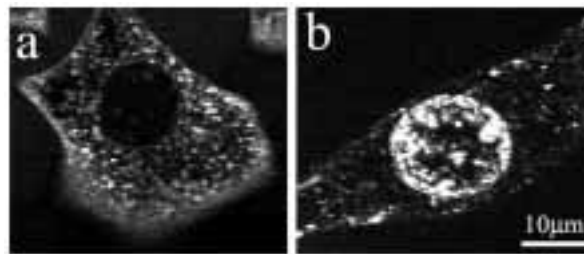

Fig. 3. (a) THG image of a fixed NIH3T3 cell. While the nucleus appears dark, numerous bright spots are observed in the cell volume. (b) THG image of a NIH3T3 cell, in which the nucleus membrane was labelled by 10nm gold nanoparticles followed by silver enhancement.

ticles were added to the growing medium about 3.5 hours prior to measurement, and entered the cell by endocytosis. In order to avoid damage to the cell we further reduced the average power of the laser to about 3mW. A plasmon-resonance TPAF image of this cell (yellow), is superimposed on a simple transmission image (blue). Note the absence of gold aggregates within the two nuclei, and the relatively large concentration between them.

A typical THG image of a fixed NIH3T3 cell, without nanoparticle labeling, is shown in Fig. 3(a). As can be seen, the nucleus appears dark, while numerous bright organelles are observed within the cell volume. In taking this image, the average laser power was about 30mW. Since THG is usually a nonresonant process, it lacks the ability for specific imaging. However, using nanoparticle labeling it is possible to specifically enhance THG. Shown in Fig. 3(b) is a THG image of a cell whose nucleus membrane was labelled with gold particles. Fixed permeabilized cells were incubated for 30 minutes in a blocking buffer, incubated overnight with Anti-tubulin cultured in Rabbit, and then incubated for two hours with Goat Anti-Rabbit IgG 10nm gold nanoparticles. Following this, the gold nanoparticles were chemically enlarged by silver enhancement. In this process silver from a silver salt solution is deposited on the gold nanoparticle, serving as a nucleation center (all in the presence of a suitable reducing agent). Since the microtubule network is not preserved during fixation, this results in labeling on receptors of the nuclear envelope. As can be seen, the nucleus appears very bright as compared with the rest of the cell, in contrast to a typical THG images of untreated cells where nuclei appear dark (Fig. 3(a)).

Shown in Fig. 4 is depth-resolved THG imaging of a NIH3T3 cell whose membrane was
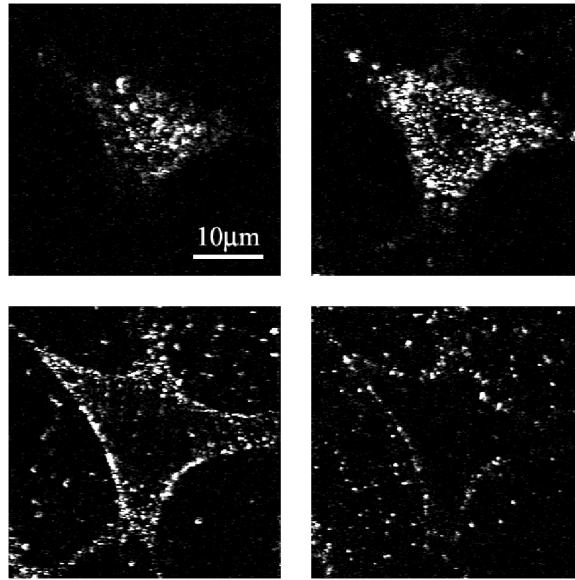
Fig. 4. Four THG sections of a NIH3T3 epithelial cell whose membrane was labelled by 10nm gold nanoparticles, followed by silver enhancement. Bright areas denote strong third-harmonic signal. The top of the cell is shown on the top left corner, while the bottom of the cell is shown on the bottom right corner. The spacing between sections is approximately $3\mu m$. The average illumination power is of the order of $1mW$. The cell shape, in the form of a triangular pyramid is clearly evident. The inside of the cell, where there are no nanoparticles, is completely dark.

labelled with silver-enhanced 10nm concanavalin-A gold particles. The sample was treated with 2% bovine serum albumin to diminish non-specific binding. Silver enhancement was performed after 1 hour incubation with gold nanoparticles. Due to the shorter incubation time and the use of the silver enhancement procedure (rather than aggregation of nanoprticles as in Figs. 1 and 2), plasmon-resonance is only achieved in sites on the external membrane of the cell. Strong THG is observed only from regions on the cell membrane. The cell is of a pyramidal shape, where the narrow top lies above the nucleus. The average laser power was about 1mW, an order of magnitude lower than typically used for THG microscopy. Therefore, no signal is observed from inside the cell, nor even from the glass surface at the bottom of the cell.

Both autofluorescence and THG occur intrinsically in cells, and are thus non-specific. Moreover, autofluorescence is usually considered an unwanted background noise in fluorescence measurements. Unlike conventional fluorescent labeling, where the measured signal originates from the label, plasmon-resonance labeling with nanoparticles relies on the enhancement of the multiphoton processes originating in the region of the cell near the nanoparticle, and not from the nanoparticle. This can be advantageous especially when the intrinsic signal varies within the cell. For example, plasmon-resonance microscopy with vibrationally resolved multiphoton processes such as coherent anti-Stokes Raman or hyper-Raman can provide chemical information on the molecular structure in the vicinity of the nanoparticles.

In general, multiphoton plasmon-resonance microscopy can be performed using a variety of laser sources and nano-labels. The optimal excitation wavelength depends both on the multiphoton process involved and on sample properties. Long wavelength lasers are preferred for highly scattering samples or when a large penetration depth is required. Shorter excitation wavelengths are often preferred in order to avoid absorption in water. As is obvious from the present work, however, the main issue is the achievement of plasmon resonance conditions for the excitation wavelength using small enough nanoparticles. This is a formidable task when using near-infrared excitation. While this resonance condition can be matched by aggregation of

small nanoparticles or by their chemical enlargement, as demonstrated above, relying on these process for bioimaging is problematic.

There seem to be, however, two alternatives, allowing the optical detection of a single, untreated, small metal nanoparticle. One is the use of a shorter wavelength (around $\lambda = 550nm$) for the excitation, requiring a much smaller particle size to achieve resonance conditions. The other is to use engineered nanoparticles, such as nanoshells and nanorings, to achieve resonance conditions in the near-infrared at a much smaller size. These should allow significantly improved quantitative imaging and multiphoton correlation spectroscopy, while avoiding photobleaching and phototoxicity.

In summary, the presented results provide a preliminary demonstration of multiphoton plasmon-resonance microscopy. This new imaging technique enables optical detection of nanometer-sized metallic particles by a nonlinear optical process, when illuminated with light in resonance with their surface plasmon. Depth resolved imaging can be accomplished by plasmon-resonance field enhancement of practically any multiphoton optical process. Specific metal nanoparticle labeling of cells is a commonly used method in electron microscopy. Plasmon-resonance microscopy can serve as a complementary method to electron microscopy, enabling simple, depth resolved imaging at optical resolution of the distribution of nanoparticles within live cells.